Crack propagation peculiarities in steels at Charpy and disc-shaped specimens tests

V.V. Kharchenko*, E.A. Kondryakov, A.V. Panasenko

G.S. Pisarenko Institute for Problems of Strength,
Nat. Ac. Sci. of Ukraine, Kyiv, Ukraine

* khar@ipp.kiev.ua

Keywords: crack propagation, crack growth rate, deformation and fracture energy, Charpy specimen, disk-shaped specimen, thermal shock.

Abstract.
An experimental technique was developed to study the propagation and arrest of cracks in Charpy specimens under impact loading and in disk-shaped specimens under thermal shock loading. Experimental and numerical simulation was conducted to determine the crack velocity in test specimens. The fracture surfaces were metallographically examined.

Introduction

Service life extension of NPP reactor pressure vessels is currently one of the critical tasks faced by the nuclear industry. Some regulatory documents [1, 2] describe techniques that account for the propagation and arrest of cracks. The search for additional strength reserves stimulates the development and improvement of various numerical and experimental techniques for analyzing the behavior (including crack propagation and arrest) of structural elements with cracks under thermal shock loading. Scaled down tests (such as the NESK-1 test [5]) conducted to study such processes require considerable expenses and do not allow complete evaluation of many factors that affect the behavior of material during crack propagation. This is why methods for testing small specimens (Charpy specimens, CT specimens, precracked disk-shaped specimens) have recently been developed [3, 4]. Such tests are relatively simple and inexpensive and provide extensive data on crack propagation and arrest.
Here we discuss the results of experimental and numerical simulation of crack propagation and arrest in Charpy specimens under impact loading and in disk-shaped specimens under thermal shock loading. The specimens are made of steel 45 and reactor steel 15Kh2NMFA.

Experimental simulation

The experimental procedure used to test precracked disk-shaped specimens under thermal shock loading was developed at the G.S. Pisarenko Institute for Problems of Strength. The specimens had dimensions d1 = 60 mm, d2 = 110 mm, h = 10 mm. A Testronic resonant testing machine (RUMUL, Switzerland) was used to grow a fatigue crack of length lcr ≈ 13 mm on the external side of the specimens.
The tests were conducted on an FP-100 testing machine equipped with facilities for heating and cooling the specimens and monitoring their temperature. The tests were performed as

follows. After preparation (welding of thermocouples, bonding of resistance strain gages, etc.), a specimen was cooled down to temperature of liquid nitrogen in a cooling chamber. Then, the cooled specimen was placed on a heat-resistant substrate and heated by pouring molten lead overheated to a temperature of ~900 °C into the central hole. This made it possible to provide the required temperature gradient and to cause the crack propagation.

The surface temperature of the specimens was monitored with thermocouples and automatic recording system, both described below. To produce a thermal shock, a special metal was melted in a crucible in the FP-100 furnace. The temperature of the melt was measured with a chromel–alumel thermocouple. The obtained data on the variation in the temperature on the outside and inside surfaces of the disk and at the crack tip were used in calculations to establish the thermomechanical loading conditions [6].

The crack velocity was measured using a 1-RDS22 crack propagation gage (made by HBM), a specially designed sensor based on KF-5 resistance strain gages, and an ADLink 9812 multichannel high-velocity analog-to-digital converter with a maximum sampling rate of 20 MS/s. The gages were bonded on the outside surface of the specimen. While extending, the crack breaks conductors of the gage and, thus, changes its resistance. The varying resistance of the gage was recorded to determine the following crack propagation parameters: place and time of crack initiation and arrest; crack velocity in steps determined by the ADLink-9812 sampling rate and the distance between conductors of the gage.

Precracked disk-shaped specimens were tested to measure the temperature at different points on their surface and the crack velocity.

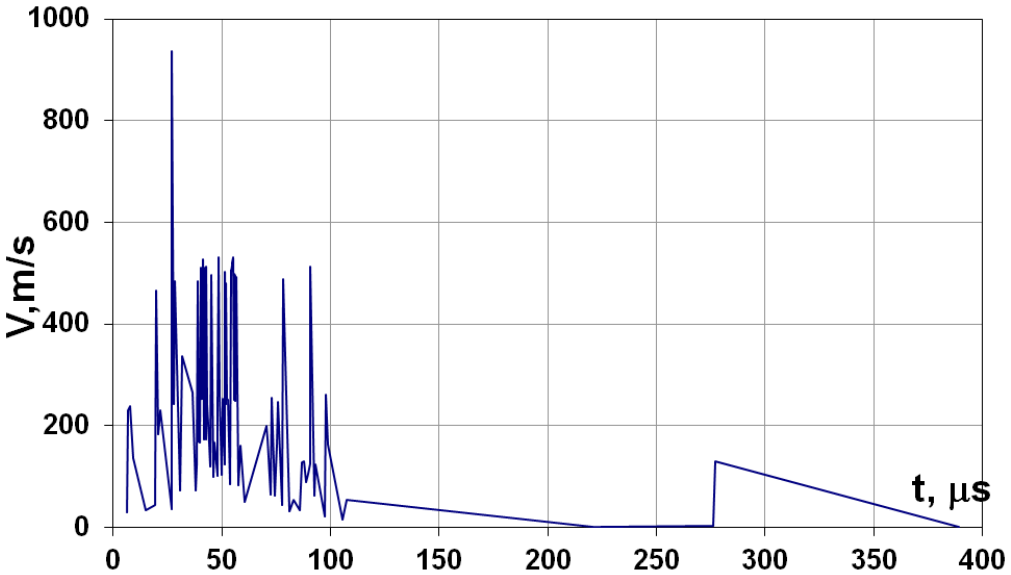

Fig. 1. Variation in crack velocity in disk-shaped steel-45 specimen with time.

After initial slow growth, the crack velocity abruptly increases to ~1000 m/s, then decreases to 300 m/s, and, after than, remains at this level until the crack is arrested (Fig. 1). This behavior of the crack velocity is in agreement with the results of numerical simulation [6] and with the results of similar tests [3, 4].

The above technique was also used to record the crack velocity in Charpy specimens subject to impact loading. The impact bending tests of standard Charpy specimens were

conducted on an instrumented drop weight impact testing machine designed and fabricated at the G.S. Pisarenko Institute for Problems of Strength [7]. The specimens were made of steel 45.

The technique and special crack gages were used to record the crack velocity as a function of crack length and time. The load on the striker was recorded as well. All parameters were recorded synchronously, which made it possible to observe the variation in the crack velocity on various sections of the force–time curve P(t). In total, 12 specimens were tested. A prepared specimen is shown in Fig. 2.

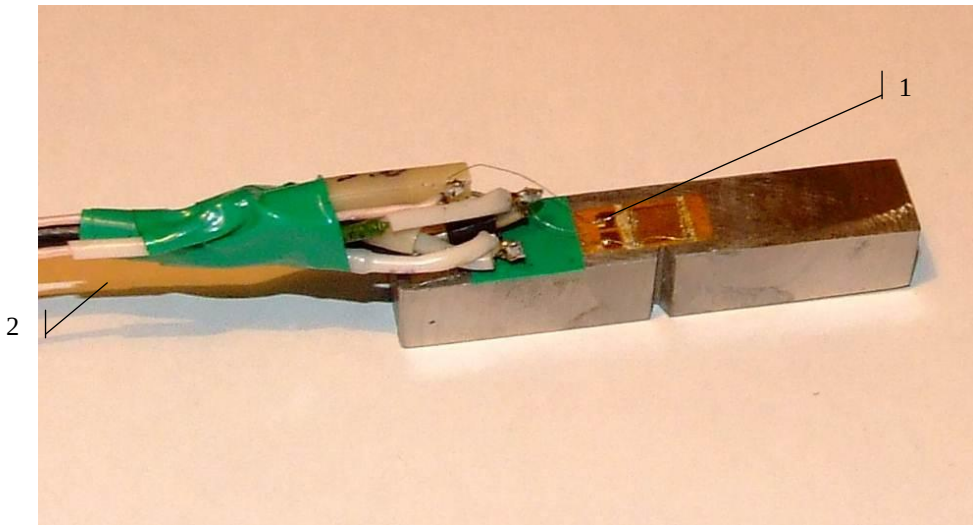

Fig. 2. Charpy specimen prepared for testing

Figure 3 shows the crack velocity in Charpy specimen as a function of time. It can be seen that the crack velocity demonstrates similar behavior in disk-shaped and Charpy specimens.

Numerical simulation.

The impact tests on Charpy specimens and the thermal-shock tests on disk-shaped specimens were numerically simulated using the finite-element method and the Gurson–Tvergaard–Needleman (GTN) damage model [8, 9]. This model describes the behavior of ductile porous materials, including the nucleation and growth of pores and ductile fracture due to their coalescence. This model may also help to describe the quasibrittle fracture of materials [10]. The model includes nine parameters. The parameters f_c and f_F are responsible for the onset of fracture and the loss of load-carrying capacity in a local region of the material, where f_c is the critical pore volume at which pores begin to coalesce within an elementary volume and f_F is the critical pore volume at which an elementary volume loses its load-carrying capacity.

Characteristics of steel 45 and steel 15Kh2NMFA were used in the calculations. The true stress–strain curves used in the numerical simulation were plotted from uniaxial-tension test data for smooth specimens.

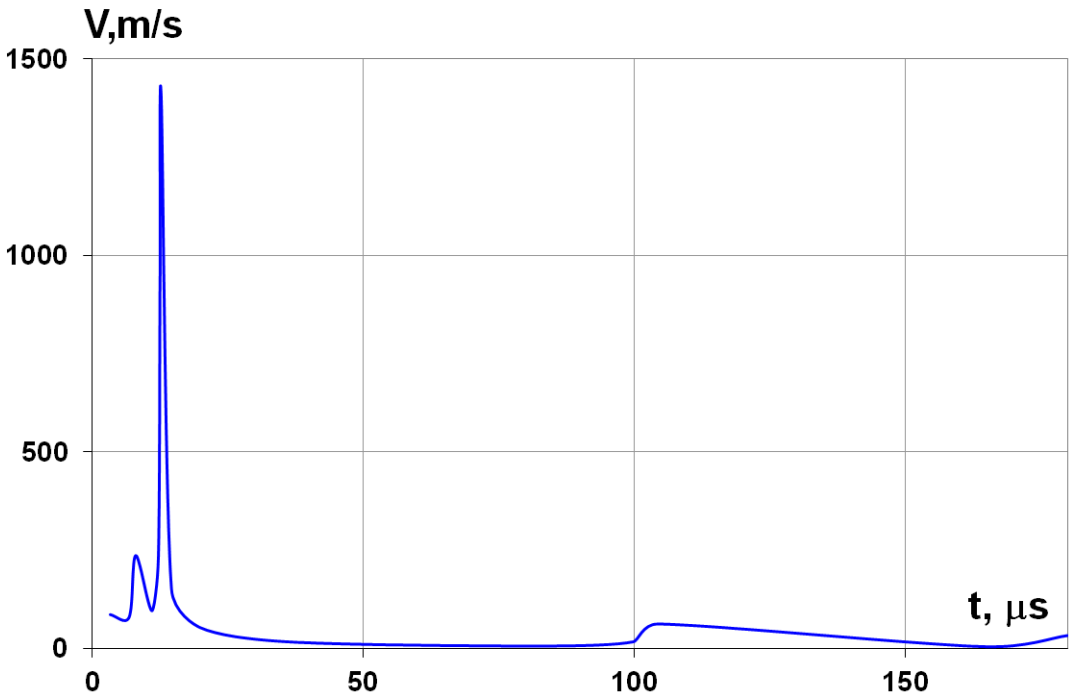

Fig. 3. Variation of crack velocity in Charpy specimen with time

The parameters of the GTN model were determined in independent uniaxial-tension tests on smooth and notched specimens. Such tests, however, fail to provide correct evaluation of the parameters f_c and f_F, which are related to the initiation and propagation of a crack. Therefore, these parameters were determined by comparing (as recommended in [11]) the crack propagation sections of theoretical and experimental force–time curves P(t). As an example, Fig. 4 compares experimental and numerically predicted force–time curves P(t).

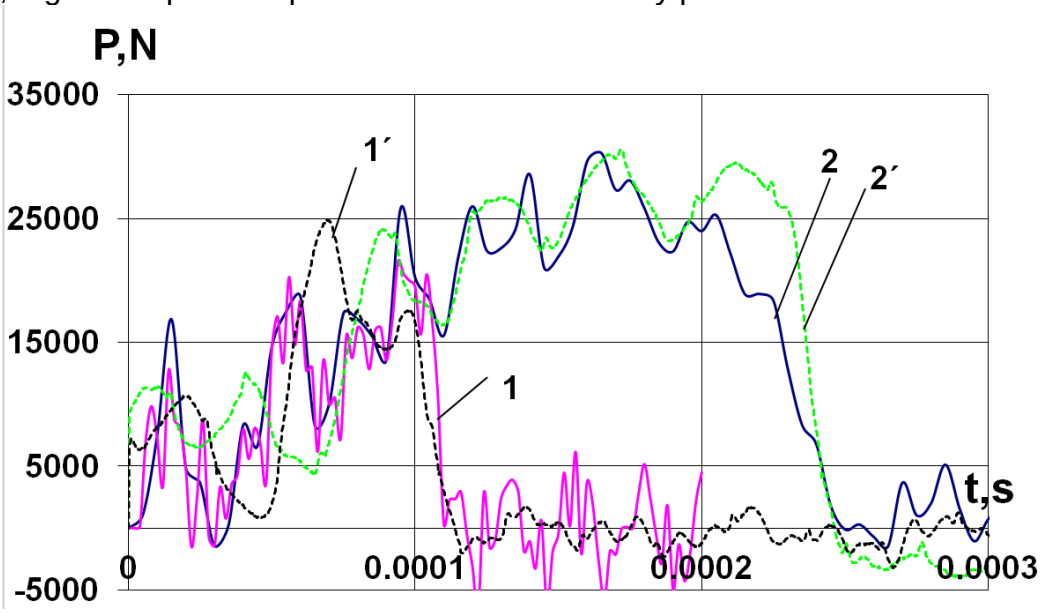

Fig. 4. Typical force–time curves for f_c = 0.0025, f_F = 0.05 (curve 1′) and f_c = 0.005, f_F = 0.05 (curve 2′) compared with experimental curves P(t) for 15Kh2NMFA steel specimens No. 410 (T =-20 °C) (curve 2) and No. 405 (T =-95°C) (curve 1) [10].

Figure 5 shows the numerically predicted time dependence of the crack velocity in a Charpy specimen under impact loading and in a disk-shaped specimen under thermal shock loading. As can be seen, the theoretical and experimental curves of crack velocity versus time are in good agreement (Figs. 1, 3, 5).

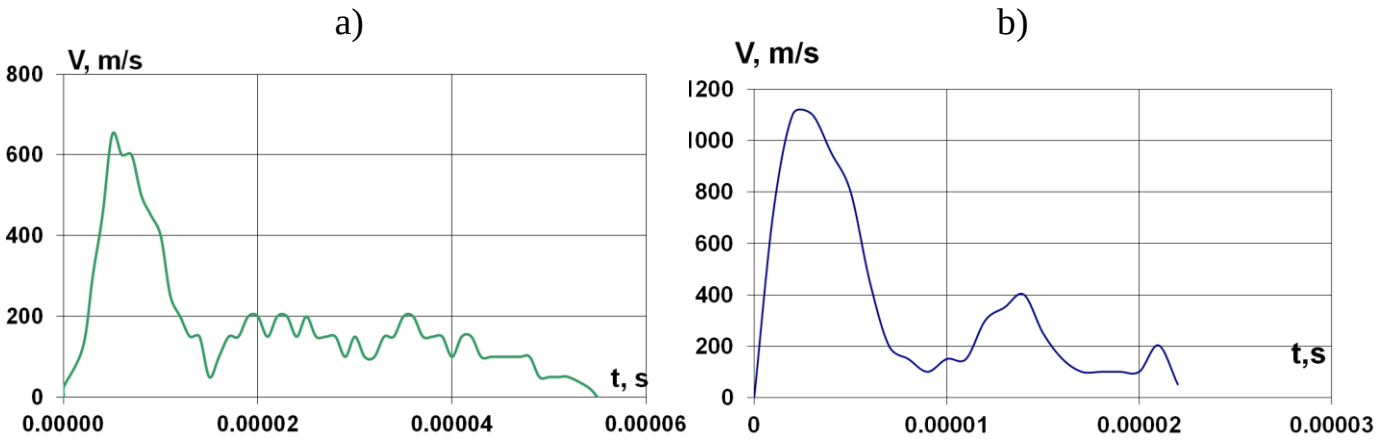

Fig. 5. Crack propagation velocity versus time for steel 15Kh2NMFA: (a) in disk-shaped specimen under thermal shock loading and (b) in Charpy specimen under impact loading

Metallographic examination

To study in detail how the crack propagates in Charpy and disk-shaped specimens, their fracture surfaces were fractographically examined with a Carl Zeiss Axiotech-100 optical microscope. Macroimages of fractures are shown in Fig. 6.

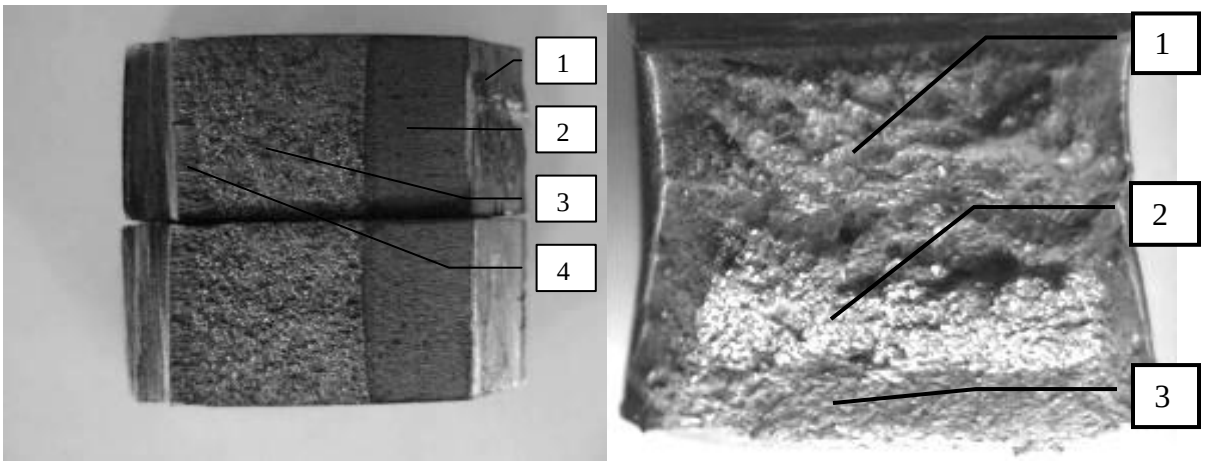

Fig. 6. Microimages of fracture in (a) disk-shaped specimen and (b) Charpy specimen.

The fractographic examination has revealed several typical areas on the fracture surfaces. Charpy specimen: 1 — ductile crack growth area; 2 — brittle fracture (crack jump) area; 3 — ductile fracture area (Fig. 6b). On some fractures, all the areas can be seen with the naked eye or at low (X 4–7) magnification. Narrow micron-scale areas and topographic features of the fracture surface can only be made out with an electronic microscope. Disk-shaped specimen: 2 — fatigue precracking area; 3 — cleavage crack jump area; 4 — ductile fracture area (Fig. 6a).

To quantify the characteristics of the objects observed on the fracture surface, we developed a fracture analysis procedure.

Each halftone image (fragment) cut out from the panorama was analyzed using a specially developed and numerically implemented cluster (segmentation) analysis algorithm.

An example of the processing of a panorama fragment is presented in Fig. 7. Figure 7a demonstrates the initial image, while Fig. 7b shows color-coded masks of objects in the image processed by the cluster-analysis algorithm. For each fragment, the distance (x) from the crack initiation site (fatigue region) was determined.

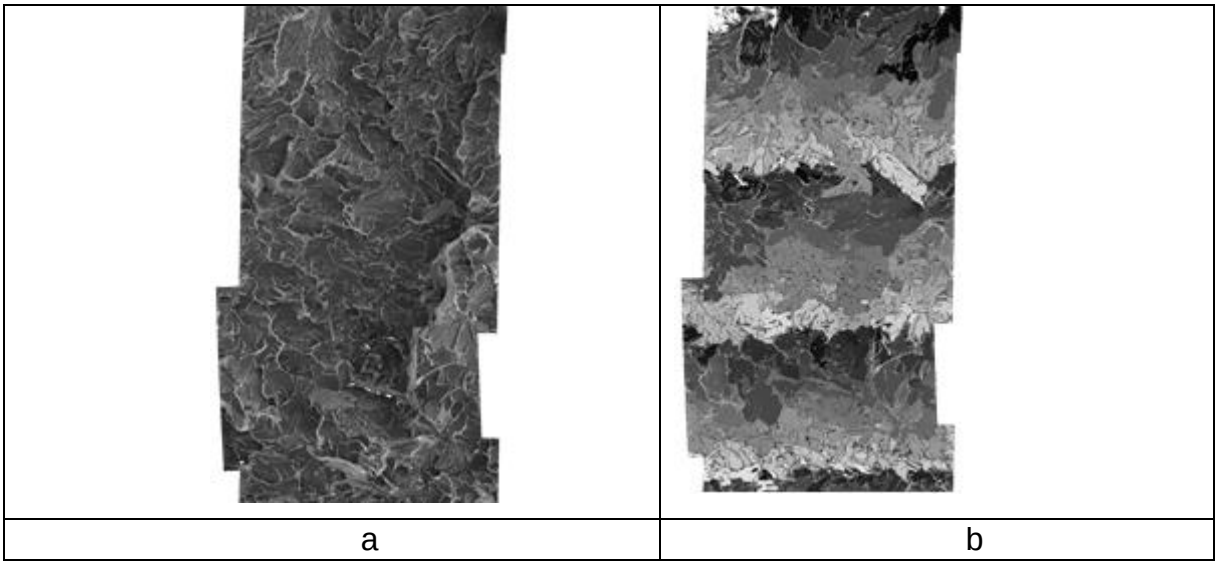

a b

Fig. 7 Fracture panorama fragments: (a) initial image, (b) color-coded masks of objects in the segmented image.

The quantitative fractographic analysis of the panorama images for steel 45 sheets and steel 45 rounds is in good agreement with the strain-gage measurement of the crack velocity.

The results from such studies were used to determine the crack parameters needed to calculate the crack velocity.

Conclusions

1. A technique for measuring the crack velocity in Charpy and disk-shaped specimens has been developed. New data on the behavior of the crack velocity in steels 45 and 15Kh2NMFA have been obtained. It has been established that the maximum crack velocity can be higher than 1000 m/s.

2. Impact tests on Charpy specimens and thermal-shock tests on disk-shaped specimens have been numerically simulated using the GTN damage model. The theoretical and experimental curves of crack velocity versus time are in good agreement.
3. To measure the parameters of the crack, the fracture surfaces of the specimens were metallographically examined. A software package for image processing and quantification of structural changes caused by a propagating crack has been developed and tested.

References

[1] Pressurized Thermal Shock in Nuclear Power Plants: Good Practices for Assessment // IAEA-TECDOC-1627. – Vienna. – 2010. – 229 p.
[2] Unified Procedure for Lifetime Assessment of Components and Piping in WWER NPPs ("VERLIFE"), European Comission. – 2008.
[3] B. Prabel, S. Marie, A. Combescure Using the X-FEM method to model the dynamic propagation and arrest of cleavage cracks in ferritic steel // Eng Fract Mech. – 2008. - Vol. 75, №10. - P. 2984–3009.
[4] C. Berdin, M. Hajjaj, Ph. Bompard [et al.] Local approach to fracture for cleavage crack arrest prediction // Eng Fract Mech. – 2008. – Vol. 75, №11. – P. 3264-3275.
[5] R. Hurst, N. Taylor, D. McGarry et al. Evaluating the NESK-1 test and the integrated approach to structural integrity assessment // Int. J. Press. Vess. and Piping. – Vol.78. – 2001. – p. 213-224.
[6] E. A Kondryakov, "Numerical simulation of crack propagation in a disk-shaped specimen under thermal shock loading," in: Reliability and Service Life of Machines and Structures [in Russian], issue 32, Naukova Dumka, Kyiv (2009), pp. 194–201.
[7] V. V. Kharchenko, E. A. Kondryakov, V. N. Zhmaka, and A. A. Babutskii, "Instrumented impact testing machine: Basic components and performance analysis," in: Reliability and Service Life of Machines and Structures [in Russian], issue 27, Naukova Dumka, Kyiv (2006), pp. 121–130.
[8] Gurson A.L. Continuum theory of ductile rupture by void nucleation and growth: Part I– Yield criteria and flow rules for porous ductile media // J. Eng. Mater. Tech. – 1977. – Vol. 99, №1. – P. 2–15.
[9] Tvergaard V. On localization in ductile materials containing spherical voids // Int. J. Fract. – 1982. - Vol. 18, № 4. - P. 237-252.
[10] E. O. Kondryakov, Initiation and Propagation of Cracks at a Stress Concentrator in Steels under Impact Loading [in Ukrainian], Author's Abstract of PhD Thesis, Kyiv (2009).
[11] Emrich A., Muhlich U.M., Kuna M. [et al.] // Indirect measuring of crack growth by means of a key-curve-method in pre-cracked Charpy specimens made of nodular cast iron / // Int. J. Fract. – 2007. - Vol. 145. - P. 47-61.